Volume 60
Number 11
7 February 2024
Pages 1351–1498

ChemComm

Chemical Communications

rsc.li/chemcomm

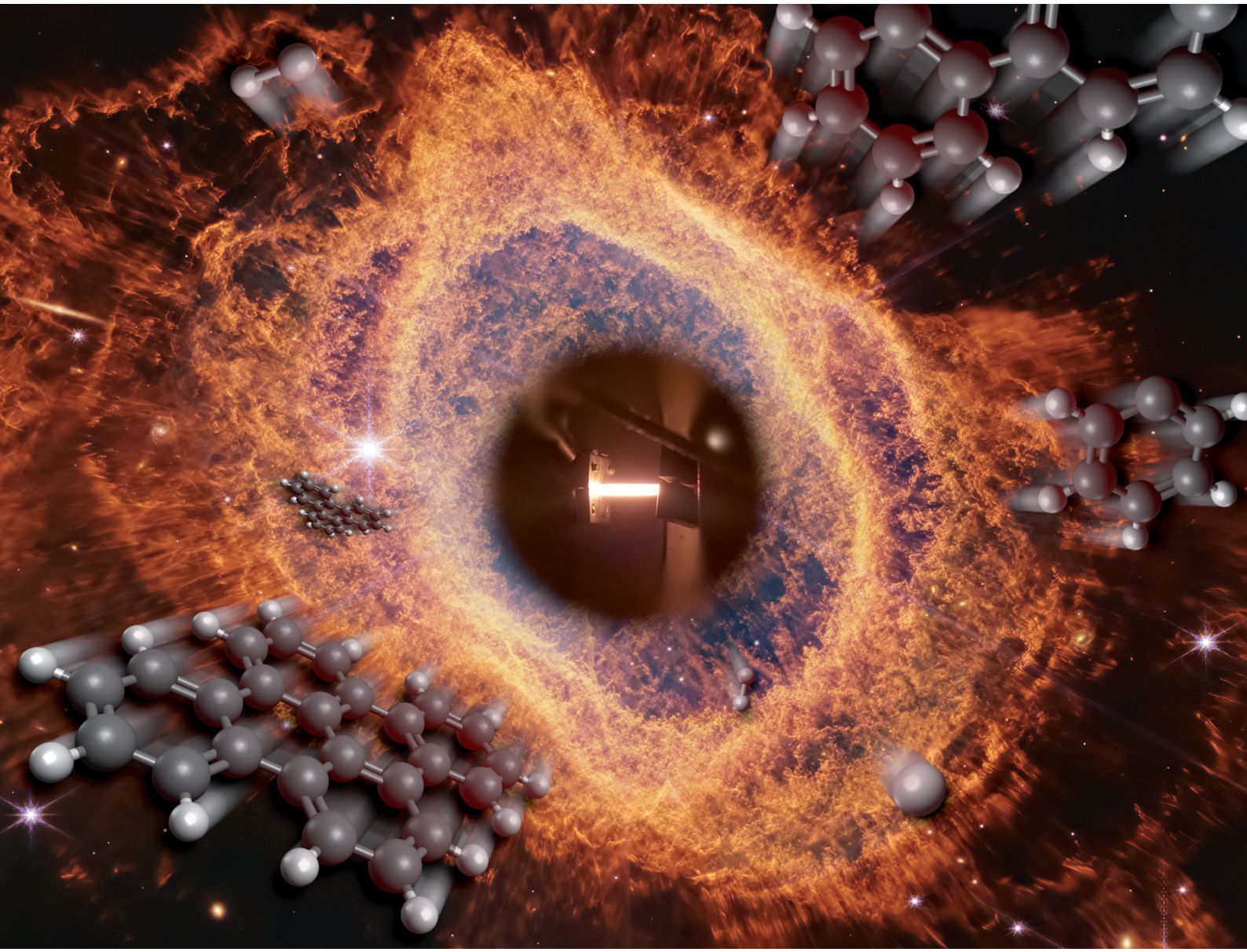

ISSN 1359-7345

ROYAL SOCIETY OF CHEMISTRY

COMMUNICATION

Agnes H. H. Chang, Patrick Hemberger, Ralf I. Kaiser *et al.* Gas-phase preparation of the dibenzo[*e,l*]pyrene ($C_{24}H_{14}$) butterfly molecule *via* a phenyl radical-mediated ring annulation

60 YEARS ANNIVERSARY

ChemComm

COMMUNICATION

Cite this: *Chem. Commun.*, 2024, **60**, 1404

Received 3rd November 2023,
Accepted 30th November 2023

DOI: 10.1039/d3cc05371g

rsc.li/chemcomm

Gas-phase preparation of the dibenzo[*e*,*l*]pyrene ($C_{24}H_{14}$) butterfly molecule *via* a phenyl radical-mediated ring annulation†

Shane J. Goettl,[a] Andrew M. Turner,[a] Bing-Jian Sun,[b] Agnes H. H. Chang,*[b] Patrick Hemberger*[c] and Ralf I. Kaiser*[a]

A high temperature phenyl-mediated addition–cyclization–dehydrogenation mechanism to form peri-fused polycyclic aromatic hydrocarbon (PAH) derivatives—illustrated through the formation of dibenzo[*e*,*l*]pyrene ($C_{24}H_{14}$)—is explored through a gas-phase reaction of the phenyl radical ($C_6H_5^{\bullet}$) with triphenylene ($C_{18}H_{12}$) utilizing photoelectron photoion coincidence spectroscopy (PEPICO) combined with electronic structure calculations. Low-lying vibrational modes of dibenzo[*e*,*l*]pyrene exhibit out-of-plane bending and are easily populated in high temperature environments such as combustion flames and circumstellar envelopes of carbon stars, thus stressing dibenzo[*e*,*l*]pyrene as a strong target for far-IR astronomical surveys.

Since the first synthesis of the 24-π dibenzo[*e*,*l*]pyrene ($C_{24}H_{14}$) molecule by Sako in 1934,[1] pyrenes—derivatives of peri-fused polycyclic aromatic hydrocarbon (PAH) pyrene ($C_{16}H_{10}$, **1**) (Fig. 1) carrying four fused benzene rings—have garnered considerable attention from the physical chemistry, organic chemistry, and materials science communities due to their optoelectronic properties as organic semiconductors and metal-free sensitizers in dye sensitized solar cells (DSSCs), and their potential incorporation as a molecular electron transfer building block in lithium-ion batteries.[2] As the smallest representative of a PAH where the benzene rings are fused through more than one face, the resonance stabilization of the pyrene stem compound is considerably higher compared to its five-membered ring isomer fluoranthene ($C_{16}H_{10}$, **2**) by 56 kJ mol^{-1}.[3] Dibenzo[*e*,*l*]pyrene ($C_{24}H_{14}$, **3**), in particular, represents a fundamental molecular building block of nanotubes, graphenes, fullerenes, and two-dimensional nanoflake fragments such as ovalene ($C_{32}H_{14}$, **4**).[4]

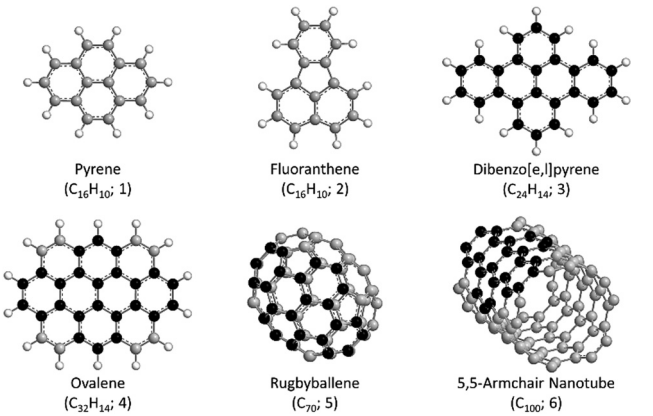

Fig. 1 Structures of pyrene (1) and fluoranthene (2), as well as dibenzo[*e*,*l*]pyrene (3), ovalene (4), rugbyballene (5), and a 5,5-armchair nanotube (6) emphasizing the potential role of dibenzo[*e*,*l*]pyrene in the formation of 2D and 3D carbonaceous nanostructures.

Its derivatives have been postulated as carriers of the unidentified infrared (UIRs) emission bands and the diffuse interstellar bands (DIBs).[5] The interstellar origin of dibenzo[*e*,*l*]pyrenes has been attributed through their detection in carbonaceous chondrites such as Allende and Murchison,[6] and sophisticated D/H and $^{13}C/^{12}C$ isotopic analyses of these meteoritic PAHs report that those PAHs were synthesized in circumstellar envelopes of carbon-rich asymptotic giant branch (AGB) stars and planetary nebulae as their descendants.[7] Overall, these surveys reveal that PAHs may encompass up to 20% of the galactic carbon budget and act as a link between resonantly stabilized free radicals and carbonaceous nanoparticles in interstellar and circumstellar environments.[8] However, astrochemical models predict the lifetimes of PAHs in the interstellar medium (ISM) to be on the order of 10^8 years, whereas the timescale for formation and injection of PAHs from carbon stars to the ISM has been derived to be on the order of 10^9 years.[9] Nevertheless, the observational arguments that PAHs are ubiquitous in interstellar and circumstellar

[a] *Department of Chemistry, University of Hawai'i at Mānoa, Honolulu, HI 96822, USA. E-mail: ralfk@hawaii.edu*
[b] *Department of Chemistry, National Dong Hwa University, Shoufeng, Hualien 974, Taiwan. E-mail: hhchang@gms.ndhu.edu.tw*
[c] *Paul Scherrer Institute, CH-5232, Villigen, Switzerland. E-mail: patrick.hemberger@psi.ch*

† Electronic supplementary information (ESI) available. See DOI: https://doi.org/10.1039/d3cc05371g

environments implies hitherto unexplored routes to their rapid chemical growth, where formation of dibenzo[*e,l*]pyrene represents a key step in molecular mass growth processes toward large PAHs and two-dimensional (2D) carbonaceous nanostructures (Fig. 1). This scenario resembles the largely incomplete set of formation mechanisms to PAHs in terrestrial combustion settings, where these species, comprised entirely of carbon and hydrogen oriented in fused benzene rings, are formed as the result of incomplete combustion processes.[10]

On Earth, the synthesis of dibenzo[*e,l*]pyrene has been accomplished in a multitude of ways. Classical approaches involve oxidative or eliminative photocyclization[11] of (un)substituted biphenyl and quaterphenyl species.[12] More recent synthetic methods utilize intramolecular aryl–aryl coupling *via* alumina-mediated high-frequency zipping,[13] annulation of cyclic diarylodonium salts,[14] *in situ* aryl–aryl coupling on silver surfaces under ultra-high vacuum (UHV) conditions,[15] and annulative dimerization of chloro- and iodobiaryl compounds.[16] However, despite the impressive progress on the preparative synthesis of dibenzo-[*e,l*]pyrene, the fundamental reaction mechanisms of molecular mass growth processes leading to and incorporating dibenzo-[*e,l*]pyrene under extreme conditions of a few 1000 K relevant to, *i.e.*, combustion flames and circumstellar envelopes of carbon-rich AGB stars, have yet to be explored. Both astrochemical and combustion chemistry models favor bottom-up molecular mass growth processes of PAHs involving low molecular weight precursors such as acetylene (C_2H_2) through successive hydrogen abstraction–acetylene addition (HACA) reactions.[17] These proceed *via* hydrogen abstraction from an aromatic hydrocarbon by a hydrogen atom followed by acetylene addition and subsequent hydrogen loss.[18] The HACA mechanism has been explored experimentally for the formation of relatively small PAHs, such as naphthalene ($C_{10}H_8$), phenanthrene ($C_{14}H_{10}$), and pyrene ($C_{16}H_{10}$).[19] Nevertheless, the HACA mechanism faces severe shortcomings such as cyclization to pentafused rings as in acenaphthylene ($C_{12}H_8$)[20] rather than addition of a second ring acetylene molecule and formation of anthracene ($C_{14}H_{10}$). Notably, flame[21] as well as astrochemical[9,22] models infer that a stepwise addition of acetylene leading to complex PAHs is too slow to account for the observed quantities of PAHs in combustion flames and meteorites. Shukla *et al.* and Xiong *et al.* postulated that a phenyl addition–dehydrocylization (PAC) pathway could cause a rapid molecular mass growth in PAHs since successive reactions of three C2 building blocks (acetylene, C_2H_2) could be efficiently replaced by a single collision with a single C6 building block (phenyl, $C_6H_5^{\bullet}$).[23] Here, PAC might involve the addition of a phenyl radical to an aromatic hydrocarbon at a three- or four-carbon bay, followed by hydrogen atom loss, dehydrogenation, cyclization, a second hydrogen atom loss, and aromatization.[18] However, a directed gas phase synthesis targeting dibenzo[*e,l*]pyrene ($C_{24}H_{14}$) through the PAC route has been elusive until now.

Herein, we report on the facile gas-phase preparation of the D_{2h} symmetric dibenzo[*e,l*]pyrene molecule ($C_{24}H_{14}$)—a hexacyclic benzenoid PAH—initiated through the bimolecular reaction of the phenyl radical ($C_6H_5^{\bullet}$) with triphenylene ($C_{18}H_{12}$) at temperatures relevant to circumstellar envelopes and combustion flames. Briefly, a high temperature chemical microreactor was exploited to prepare the dibenzo[*e,l*]pyrene molecule ($C_{24}H_{14}$) *via* the gas-phase reaction of the phenyl radical ($C_6H_5^{\bullet}$) with triphenylene ($C_{18}H_{12}$). Exploiting molecular beam experiments with isomer-selective photoelectron photoion coincidence (PEPICO) spectroscopy[24] and tunable vacuum ultraviolet (VUV) photoionization combined with *ab initio* electronic structure calculations, the gas phase formation of dibenzo[*e,l*]pyrene showcases the PAC mechanism as a versatile, efficient pathway involved in the synthesis of large PAHs, which may serve as fundamental building blocks for two- or three-dimensional carbonaceous nanostructures in combustion flames and circumstellar environments at the molecular level (Fig. 1).

Fig. 2 shows a representative mass spectrum for the reaction of the phenyl radical ($C_6H_5^{\bullet}$; 77 amu) with triphenylene ($C_{18}H_{12}$; 228 amu) recorded at a photoionization energy of 9.00 eV at 300 K (no pyrolysis) (Fig. 2a) and 1200 ± 100 K (pyrolysis ON) (Fig. 2b). In both cases, prominent ion counts were observed at mass-to-charge (m/z) ratios of 228 ($C_{18}H_{12}^{+}$) and 229 ($^{13}CC_{17}H_{12}^{+}$). The former peak corresponds to the triphenylene precursor ($C_{18}H_{12}$; 228 amu), while the latter can be attributed to ^{13}C-substituted triphenylene ($^{13}CC_{17}H_{12}$; 229 amu) at an abundance of about 20% to account for the 1.1% natural abundance of ^{13}C. Under pyrolysis conditions (Fig. 2b), new peaks arise at m/z = 302 ($C_{24}H_{14}^{+}$) and 304 ($C_{24}H_{16}^{+}$), which are not present without the pyrolysis at 300 K. The signal at m/z = 304 indicates the formation of $C_{24}H_{16}$ species, possibly the result of a phenyl addition to the C1 or C2 carbons of triphenylene followed by hydrogen atom loss. The signal at m/z = 302 provides clear evidence that the reaction of phenyl radicals with triphenylene leads to products of the molecular formula $C_{24}H_{14}$.

The formation of molecule(s) with the molecular formula $C_{24}H_{14}$ through reaction of the phenyl radical with triphenylene, as indicated in the mass spectrum, does not alone prove the selectivity towards dibenzo[*e,l*]pyrene. Thus we also elucidated

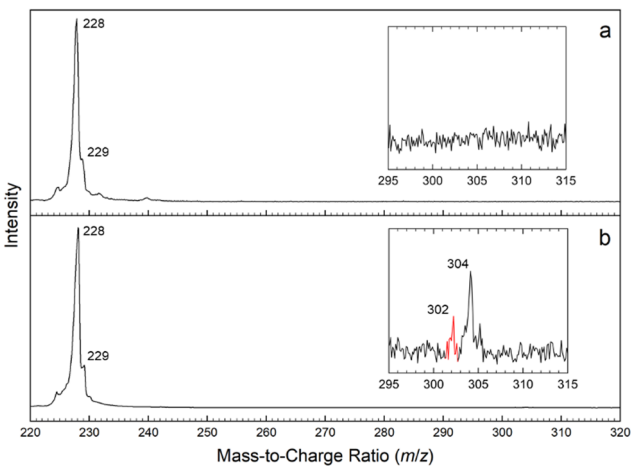

Fig. 2 Mass spectra taken at a photon energy of 9.00 eV for the nitrosobenzene–triphenylene system. (a) pyrolysis OFF; (b) pyrolysis ON at 1200 ± 100 K. The mass peak of the newly formed $C_{24}H_{14}$ (m/z = 302) species is highlighted in red.

the nature of the structural isomer(s) formed. This was accomplished by analyzing the corresponding photoionization efficiency (PIE) curves (Fig. 3a) and the mass-selected threshold photoelectron (ms-TPE) spectra (Fig. 3b) along with the reference spectrum, at m/z = 302. First, the PIE curve depicts ion counts at m/z = 302 ($C_{24}H_{14}^{+}$) as a function of photon energy from 7.00 to 10.00 eV. The reference PIE curve of the $C_{24}H_{14}$ isomer dibenzo[*e,l*]pyrene (blue) matches the phenyl–triphenylene experimental PIE curve (black) exceptionally well over the entire photon energy range with ionization onsets of 7.35 ± 0.10 and 7.31 ± 0.10 eV, respectively. The matching onsets of the ion counts along with the fits of the PIE curves indicate that the experimental data can be fit with a single isomer: dibenzo[*e,l*]pyrene ($C_{24}H_{14}$).

Second, these findings are reinforced by exploiting ms-TPE spectra (Fig. 3b), which display ion counts at m/z = 302 ($C_{24}H_{14}^{+}$) in coincidence with electrons of less than 10 meV as a function of photon energy from 7.00 to 8.50 eV. Similar to the PIE curves, both the phenyl–triphenylene experimental ms-TPES (m/z = 302) (black) and the dibenzo[*e,l*]pyrene reference ms-TPES (blue) clearly match; furthermore, in comparison to the PIE curve, the ms-TPE spectra reveal distinct structures featuring four peaks at 7.40 ± 0.05, 7.56 ± 0.05, 7.78 ± 0.05, and 8.20 ± 0.05 eV. The first, third, and fourth peaks can be assigned to the $3b_{3g}$, $3b_{2g}$, and $2a_u$ states, respectively, while the second is due to the vibrational transitions from the ground cationic state.[25] To elucidate the vibrational features, we performed Franck–Condon (FC) spectral modeling, depicted also in Fig. 3b. The transitions into the ions' ground state ($3b_{3g}$) show activity of three ring deformation modes at 314, 660 and 1274 cm^{-1}, respectively, which are responsible for the feature at 7.56 eV. While for the $3b_{3g}$ and $2a_u$ states we found planar cationic structures and only low activity of ring deformation modes associated with a smaller change in geometry upon ionization, the $3b_{2g}$ cation state shows a significant out-of-plane deformation. This leads to a symmetry reduction (C_{2v}) that translates into activity of a low lying out-of-plane vibrational mode (26 cm^{-1}) upon ionization, reminiscent of a butterfly in flight, and a much denser spectrum with contributions from sequence band transitions even at 300 K vibrational temperatures. Overall, combining the results from the PIE curves, the ms-TPE spectra, and the FC simulations provide clear evidence for the formation of dibenzo[*e,l*]pyrene in the phenyl–triphenylene system.

Now that the gas-phase formation of dibenzo[*e,l*]pyrene from the reaction of phenyl radicals with triphenylene has been explicitly confirmed experimentally, the reaction mechanisms leading to dibenzo[*e,l*]pyrene are also untangled computationally. This is accomplished by exploiting electronic structure calculations in conjunction with the experimental results to explore the reaction pathways (Fig. 4) (ESI†). All energies referred to in this section are with respect to separated reactants. The CCSD(T)/cc-pVDZ//B3LYP/cc-pVTZ level calculations predict phenyl radical addition to the C1 carbon of triphenylene proceeding over a small entrance barrier of 10 kJ mol^{-1} to intermediate [**i1**] which is stabilized by 129 kJ mol^{-1}. Phenyl addition to the C2 carbon of triphenylene is shown in Fig. S3 (ESI†), but cannot lead to dibenzo[*e,l*]pyrene (**p1**). The synthetic pathway to **p1** involves [**i1**] *via* hydrogen atom loss from the attacked carbon through a 35 kJ mol^{-1} barrier to form [**i2**] residing at 23 kJ mol^{-1} below the separated reactants. From here, the reaction progresses to **p1** through two possible routes: [**i2**] → [**i3**] → [**i5**] → **p1** and [**i2**] → [**i4**] → [**i6**] → **p1**. These pathways involve first a hydrogen abstraction by a hydrogen atom from either the C2 carbon of the phenyl moiety or the C12 carbon of the triphenylene moiety of [**i2**] leading to [**i3**] or [**i4**], respectively. These pathways are followed by ring closure to [**i5**] or [**i6**]. The reaction is terminated through subsequent hydrogen atom elimination to **p1** accompanied by aromatization. The highest barriers in the reaction pathway stem from the hydrogen abstraction to [**i3**] and [**i4**] at 102 and 98 kJ mol^{-1}, respectively. Since the transition states are higher in energy than the separated reactants, the reaction of phenyl radicals with triphenylene eventually leading to dibenzo[*e,l*]pyrene (**p1**) can only proceed at high temperatures such as in, *e.g.*, circumstellar envelopes of carbon stars and combustion flames.

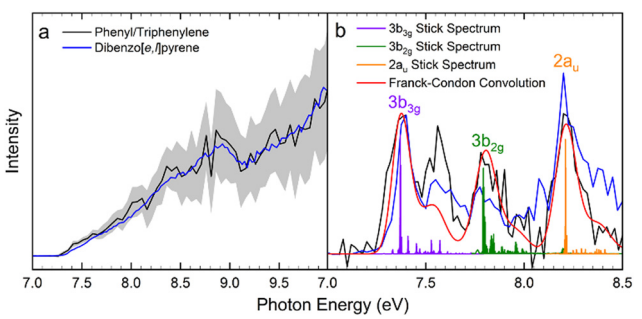

Fig. 3 PIE curves (a) and ms-TPE spectra (b) taken at m/z = 302. Black: phenyl–triphenylene experimental spectrum; blue: dibenzo[*e,l*]pyrene experimental spectrum. Molecular orbital assignments[25] and Franck–Condon stick spectra for transitions to the ground ($3b_{3g}$), first excited ($3b_{2g}$), and second excited cation states ($2a_u$) of dibenzo[*e,l*]pyrene are shown in violet, green, and orange, respectively, with a Gaussian convolution over the stick spectra shown in red. The overall error bars (gray area) consist of two parts: 1σ error of the PIE curve averaged over the individual scans and ±10% based on the accuracy of the photodiode.

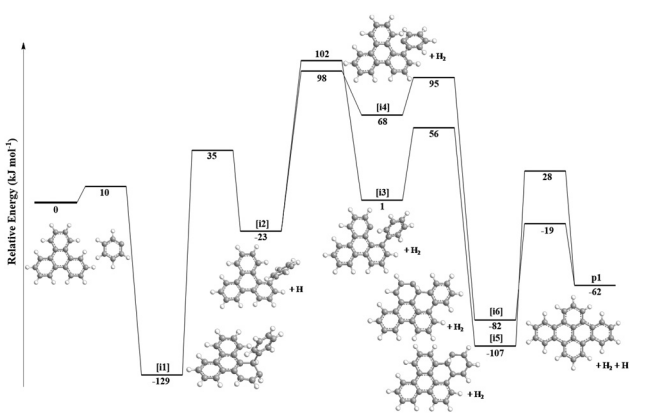

Fig. 4 Potential energy surface (PES) for the phenyl reaction with triphenylene calculated at the CCSD(T)/cc-pVDZ//B3LYP/cc-pVTZ level of theory leading to dibenzo[*e,l*]pyrene.

To conclude, our combined experimental and computational study of the gas-phase reaction of phenyl radicals with triphenylene led to the formation of dibenzo[*e*,*l*]pyrene (**p1**), a planar PAH consisting of six fused benzenoid rings arrayed in a D_{2h} symmetric "butterfly" shape. The vibrational analysis reveals dibenzo[*e*,*l*]pyrene exhibiting an out-of-plane bending mode of the outer benzene moieties (ν_1) at 7 cm^{-1} showcasing the impression of butterfly wings flapping (Movies S1 and S2, ESI†). The combined flexibility of the dibenzo[*e*,*l*]pyrene carbon skeleton—characteristic of acenes—and stability of the pyrene core increases the likelihood to participate in facile molecular mass growth processes preparing 3D structures such as rugbyballene (C_{70}) and carbon nanotubes (Fig. 1). Additionally, molecules like dibenzo[*e*,*l*]pyrene, which contain this type of "floppy" vibrational mode, can be readily excited in high temperature regions, such as planetary nebulae and circumstellar envelopes of carbon stars. This leads to high populations of vibrationally excited species producing strong infrared emission bands upon relaxation. Utilizing the Boltzmann distribution for the case of dibenzo[*e*,*l*]pyrene at a temperature of 2000 K to simulate circumstellar conditions, the population of the aforementioned vibrational mode is approximated to be very high, at about 92%. Hence, dibenzo[*e*,*l*]pyrene embodies a strong target for spectral line surveys in the far-IR wavelength range toward carbon-rich circumstellar envelopes as a representative of symmetric PAHs.

This work was supported by the U.S. Department of Energy, Basic Energy Sciences, by Grant No. DE-FG02-03ER15411 to the University of Hawaii at Manoa. The experiments have been carried out at the VUV (x04db) beamline of the Swiss Light Source (SLS) located at the Paul Scherrer Institute, Villigen Switzerland. BJS and AHHC thank the National Center for High-Performance Computing in Taiwan for providing the computer resources. Background image of the Table of Contents entry is adapted from Judy Schmidt (distributed under a CC BY license: **https://creativecommons.org/licenses/by/2.0/**).

Conflicts of interest

There are no conflicts to declare.

Notes and references

1 S.-i Sako, *Bull. Chem. Soc. Jpn.*, 1934, **9**, 55–74.
2 J. Kwon, J.-P. Hong, W. Lee, S. Noh, C. Lee, S. Lee and J.-I. Hong, *Org. Electron.*, 2010, **11**, 1103–1110; C. Aumaitre and J. F. Morin, *Chem. Rec.*, 2019, **19**, 1142–1154; Q. Li, Y. Zhang, Z. Xie, Y. Zhen, W. Hu and H. Dong, *J. Mater. Chem. C*, 2022, **10**, 2411–2430; R. Rakhi and C. H. Suresh, *ChemistrySelect*, 2021, **6**, 2760–2769; D. Wu, Z. Xie, Z. Zhou, P. Shen and Z. Chen, *J. Mater. Chem. A*, 2015, **3**, 19137–19143.
3 D. Khiri, D. Q. Dao, B. T. Nguyen, L. Gasnot, F. Louis and A. El Bakali, *J. Phys. Chem. A*, 2019, **123**, 7491–7498.
4 P. J. F. Harris, *Carbon*, 2007, **45**, 229–239; H. C. Lee, W.-W. Liu, S.-P. Chai, A. R. Mohamed, A. Aziz, C.-S. Khe, N. M. S. Hidayah and U. Hashim, *RSC Adv.*, 2017, **7**, 15644–15693; H. E. Lim, Y. Miyata, R. Kitaura, Y. Nishimura, Y. Nishimoto, S. Irle, J. H. Warner, H. Kataura and H. Shinohara, *Nat. Commun.*, 2013, **4**, 1–7; G. Mulas, A. Zonca, S. Casu and C. Cecchi-Pestellini, *Astrophys. J., Suppl. Ser.*, 2013, **207**, 7.
5 A. M. Ricks, G. E. Douberly and M. A. Duncan, *Astrophys. J.*, 2009, **702**, 301; A. Maragkoudakis, C. Boersma, P. Temi, J. D. Bregman and L. J. Allamandola, *Astrophys. J.*, 2022, **931**, 38; G. P. Van der Zwet and L. J. Allamandola, *Astron. Astrophys.*, 1985, **146**, 76–80.
6 L. Becker and T. E. Bunch, *Meteorit. Planet. Sci.*, 1997, **32**, 479–487; M. P. Callahan, A. Abo-Riziq, B. Crews, L. Grace and M. S. de Vries, *Spectrochim. Acta, Part A*, 2008, **71**, 1492–1495.
7 F. L. Plows, J. E. Elsila, R. N. Zare and P. R. Buseck, *Geochim. Cosmochim. Acta*, 2003, **67**, 1429–1436.
8 Y. M. Rhee, T. J. Lee, M. S. Gudipati, L. J. Allamandola and M. Head-Gordon, *Proc. Natl. Acad. Sci. U. S. A.*, 2007, **104**, 5274–5278; K. O. Johansson, M. P. Head-Gordon, P. E. Schrader, K. R. Wilson and H. A. Michelsen, *Science*, 2018, **361**, 997–1000.
9 E. R. Micelotta, A. P. Jones and A. G. G. M. Tielens, *Astron. Astrophys.*, 2010, **510**, A36; M. Frenklach and E. D. Feigelson, *Astrophys. J.*, 1989, **341**, 372–384.
10 S. P. Bagley and M. J. Wornat, *Energy Fuels*, 2013, **27**, 1321–1330; S. Thomas, N. B. Poddar and M. J. Wornat, *Polycyclic Aromat. Compd.*, 2012, **32**, 531–555; R. E. Winans, N. A. Tomczyk, J. E. Hunt, M. S. Solum, R. J. Pugmire, Y. J. Jiang and T. H. Fletcher, *Energy Fuels*, 2007, **21**, 2584–2593; A. Kousoku, R. Ashida, A. Miyasato, M. Miyake and K. Miura, *J. Chem. Eng. Jpn.*, 2014, **47**, 406–415.
11 F. B. Mallory and C. W. Mallory, *Org. React.*, 1984, **30**, 1–456.
12 T. Sato, S. Shimada and K. Hata, *Bull. Chem. Soc. Jpn.*, 1971, **44**, 2484–2490; P. G. Copeland, R. E. Dean and D. McNeil, *J. Chem. Soc.*, 1960, 4522–4524.
13 A. K. Steiner and K. Y. Amsharov, *Angew. Chem., Int. Ed.*, 2017, **56**, 14732–14736.
14 D. Zhu, H. Peng, Y. Sun, Z. Wu, Y. Wang, B. Luo, T. Yu, Y. Hu, P. Huang and S. Wen, *Green Chem.*, 2021, **23**, 1972–1977.
15 L. Feng, T. Wang, H. Jia, J. Huang, D. Han, W. Zhang, H. Ding, Q. Xu, P. Du and J. Zhu, *Chem. Commun.*, 2020, **56**, 4890–4893.
16 M. Uryu, T. Hiraga, Y. Koga, Y. Saito, K. Murakami and K. Itami, *Angew. Chem., Int. Ed.*, 2020, **132**, 6613–6616; C. Zhu, D. Wang, D. Wang, Y. Zhao, W. Y. Sun and Z. Shi, *Angew. Chem., Int. Ed.*, 2018, **130**, 8986–8991.
17 A. G. G. M. Tielens, *Rev. Mod. Phys.*, 2013, **85**, 1021.
18 R. I. Kaiser and N. Hansen, *J. Phys. Chem. A*, 2021, **125**, 3826–3840.
19 D. S. Parker, R. I. Kaiser, T. P. Troy and M. Ahmed, *Angew. Chem., Int. Ed.*, 2014, **53**, 7740–7744; T. Yang, T. P. Troy, B. Xu, O. Kostko, M. Ahmed, A. M. Mebel and R. I. Kaiser, *Angew. Chem., Int. Ed.*, 2016, **55**, 14983–14987; T. Yang, R. I. Kaiser, T. P. Troy, B. Xu, O. Kostko, M. Ahmed, A. M. Mebel, M. V. Zagidullin and V. N. Azyazov, *Angew. Chem., Int. Ed.*, 2017, **129**, 4586–4590; L. Zhao, R. I. Kaiser, B. Xu, U. Ablikim, M. Ahmed, D. Joshi, G. Veber, F. R. Fischer and A. M. Mebel, *Nat. Astron.*, 2018, **2**, 413–419.
20 D. S. N. Parker, R. I. Kaiser, B. Bandyopadhyay, O. Kostko, T. P. Troy and M. Ahmed, *Angew. Chem., Int. Ed.*, 2015, **54**, 5421–5424.
21 A. Raj, I. D. C. Prada, A. A. Amer and S. H. Chung, *Combust. Flame*, 2012, **159**, 500–515.
22 E. R. Micelotta, A. P. Jones and A. G. G. M. Tielens, *Astron. Astrophys.*, 2010, **510**, A37; E. R. Micelotta, A. P. Jones and A. G. G. M. Tielens, *Astron. Astrophys.*, 2011, **526**, A52.
23 B. Shukla, A. Susa, A. Miyoshi and M. Koshi, *J. Phys. Chem. A*, 2008, **112**, 2362–2369; S. Xiong, J. Li, J. Wang, Z. Li and X. Li, *Comput. Theor. Chem.*, 2012, **985**, 1–7.
24 P. Hemberger, A. Bodi, T. Bierkandt, M. Köhler, D. Kaczmarek and T. Kasper, *Energy Fuels*, 2021, **35**, 16265–16302.
25 R. Boschi, E. Clar and W. Schmidt, *J. Chem. Phys.*, 1974, **60**, 4406–4418.